Supplementary Information (SI) for Nanoscale.
This journal is © The Royal Society of Chemistry 2025

Supporting Information

Title:

High-Performance Aqueous Copper-Ion Batteries Based on Iron Hexacyanoferrate Cathode for Enhanced Energy Storage

Jinshu Zhang [a], Lexian Liu [a], Yuao Wang [c], Yantuo Li [a], Yang Yang [a], Mingyi Ning [a], Jianxue Wu [a], Bingjie Ma [a], and Wei Liu [a, b, *]

[a] School of Physics, Key Laboratory of Quantum Materials and Devices of Ministry of Education, Frontiers Science Center for Mobile Information Communication and Security, Southeast University, Nanjing 211189, China

[b] Purple Mountain Laboratories, Nanjing 211111, China

[c] Key Laboratory of Superlight Materials and Surface Technology of Ministry of Education, College of Materials Science and Chemical Engineering, Harbin Engineering University, Harbin 150001, China

[*] Corresponding authors.

E-mail addresses: 101012931@seu.edu.cn (W. Liu).

EXPERIMENTAL SECTION

Synthesis of FeHCF nanocrystals

FeHCF nanocrystals were synthesized via the coprecipitation method. First, 5.41 g of $FeCl_3$ (Meryer M25990-100G, AR, 99%) was dissolved in 330 mL of water to obtain solution A, and 5.49 g of $K_3Fe(CN)_6$ (Meryer M87020-100G, AR, ≥99.5%) was dissolved in 170 mL of water to obtain solution B. Solution A was heated to 60 °C under stirring, while solution B was added dropwise into solution A at a rate of 0.5 mL min^{-1}. The reaction was maintained at this temperature for 12 hours to ensure completion. The resulting precipitate was collected, thoroughly washed with water, and vacuum-dried at 120 °C to yield dark green FeHCF nanocrystals.

Electrochemical characterization

The FeHCF cathode was fabricated by mixing the FeHCF, super P, and polyvinylidene difluoride (PVDF) in a mass ratio of 7 : 2 : 1 in the solvent of N-methyl-2-pyrrolidone (NMP) to produce the electrode slurry, which was then casted onto carbon cloth followed by vacuum drying at 80 °C. Commercial copper or zinc sheet was directly used as anode. For Cu-FeHCF batteries, 1.0 M $CuSO_4$ solution is used for the electrolyte. The Zn//FeHCF decoupled battery was assembled in home-made battery case. The Zn//FeHCF decoupled battery was divided into three parts by cation exchange membrane (CEM, fumasep FKE-50) and anion exchange membrane (AEM, fumasep FAB-PK-130). The anode part was immersed in 1 M NaOH solution with Zn electrode, the cathode part was immersed in 1 M $CuSO_4$ solution with FeHCF electrode, and the charge balance was maintained with 1 M Na_2SO_4 solution in the middle. Cyclic voltammetry (CV) and electrochemical impedance spectroscopy (EIS) were measured on an electrochemical workstation (PGSTAT 302N, Autolab). while the rate and cycling performance, galvanostatic charge/discharge (GCD) profiles, and galvanostatic intermittent titration technique (GITT) were acquired from LAND test system. The specific capacity was calculated based on the mass of FeHCF. The Coulombic efficiency is calculated as $(\text{charge capacity}/\text{discharge capacity}) \times 100\%$.

Materials characterization

The shape and morphology of the samples were observed using scanning electron microscopy (SEM, Hitachi SU-8010). The crystalline structure of the samples was characterized by X-ray diffraction (XRD, Rigaku MiniFlex), Raman spectroscopy (Horiba Jobin Yvon, XploRA Plus) and FTIR spectroscopy (Nicolet 5700). For in-situ XRD tests, a homemade 2032-type coin cell equipped with a heat resistant tape was used. During the in-situ XRD test, X-rays pass through windows sealed with heat resistant tape and then was scattered on the FeHCF electrode. The samples were also investigated by X-ray photoelectron spectroscopy (XPS, Thermo Scientific K-Alpha).

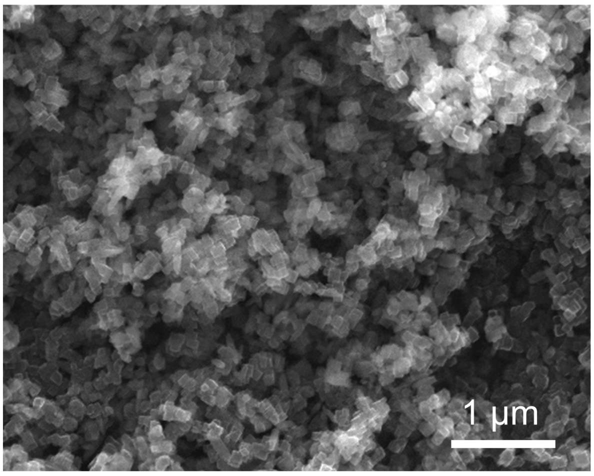

Figure S1. SEM image of FeHCF.

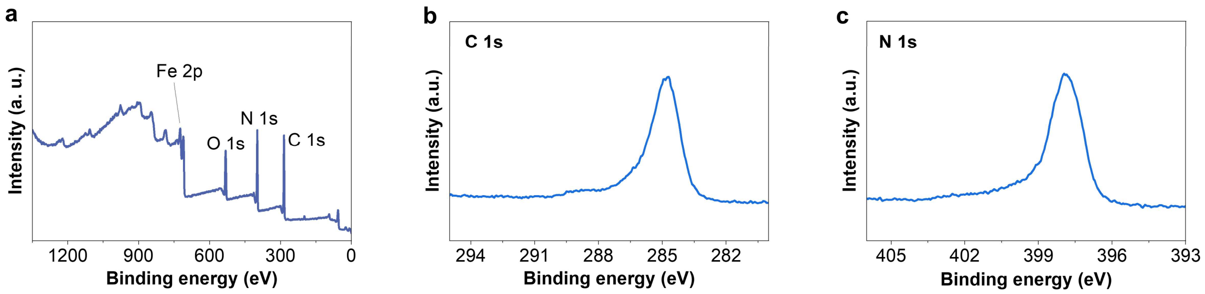

Figure S2. XPS spectra of a) survey spectrum, b) C 1s and c) N 1s for FeHCF.

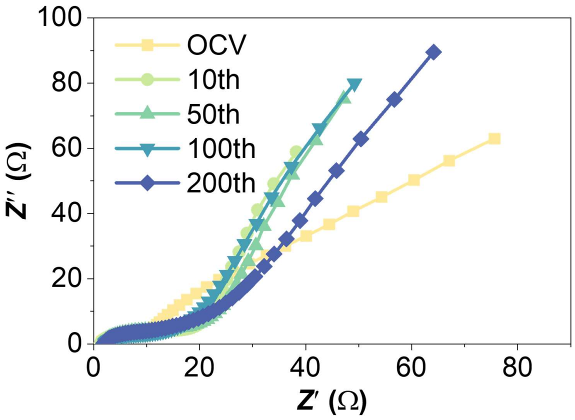

Figure S3. Impedance spectra of FeHCF electrode under different number of cycles.

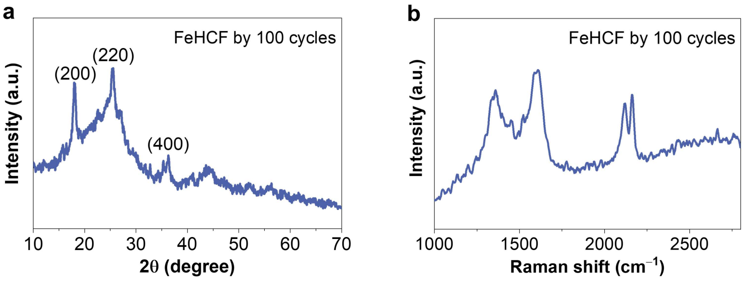

Figure S4. a) XRD patterns and b) Raman spectra of the FeHCF electrode after 100 cycles.

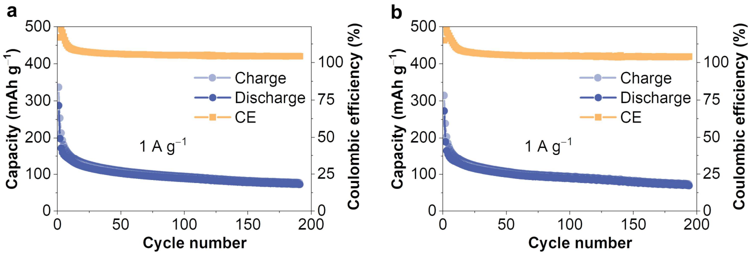

Figure S5. The electrochemical performance of electrode with different compositions: a) FeHCF : super P : PVDF = 8 : 1 : 1 and b) FeHCF : super P : PVDF = 5 : 3 : 2 in 1 M $CuSO_4$ solution.

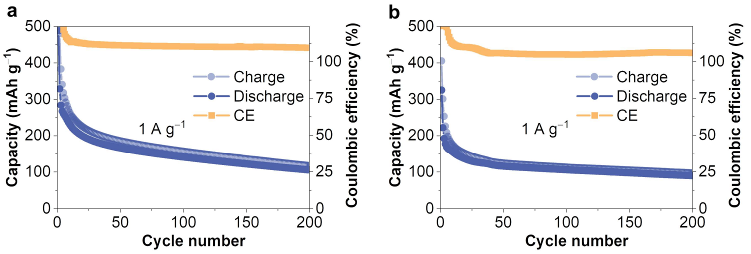

Figure S6. The electrochemical performance of the FeHCF : super P : PVDF = 7 : 2 : 1 electrode in a) 0.5 M $CuSO_4$ and b) 2 M $CuSO_4$ solution.

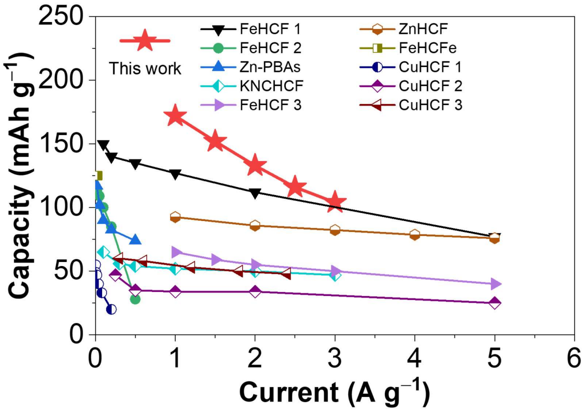

Figure S7. Comparison of FeHCF with recently reported similar electrodes.[1-10]

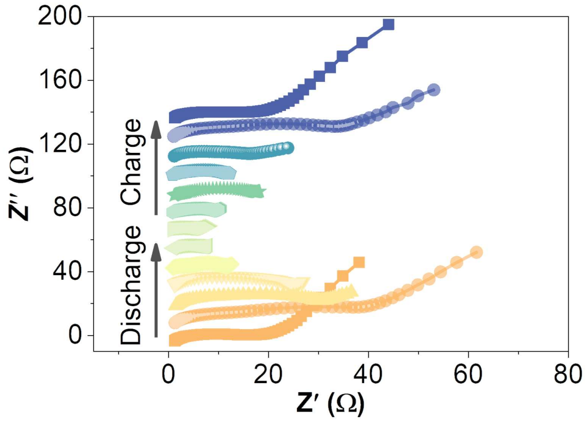

Figure S8. Impedance spectra for FeHCF electrode at various potential stages.

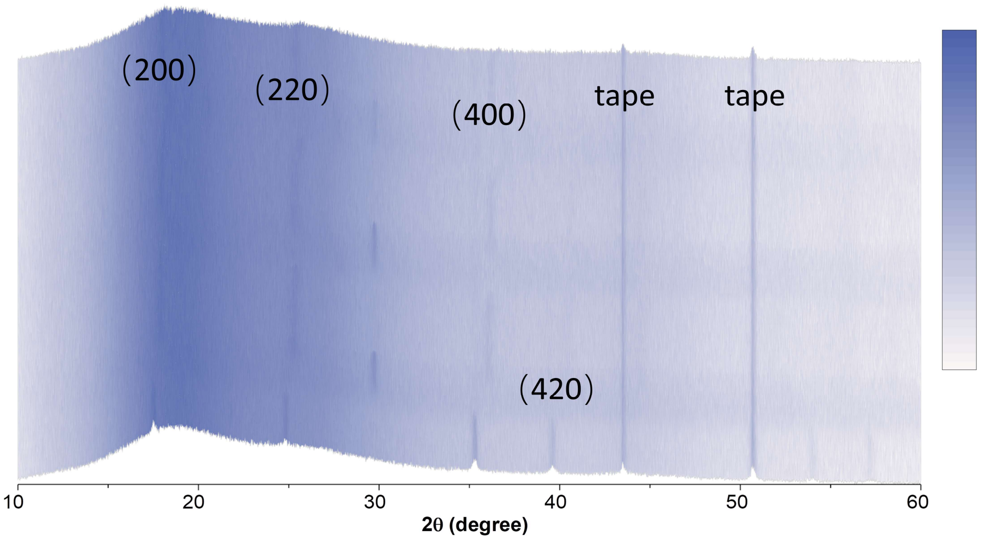

Figure S9. In-situ XRD patterns of FeHCF collected at various stages showing the structural evolution upon electrochemical copper-ion storage corresponding to Figure 4a.

References

1. Z. He, G. Wang, R. Yu, Y. Jiang, M. Huang, F. Xiong, S. Tan, M. F. L. De Volder, Q. An and L. Mai, *ACS Nano*, 2024, **18**, 17304-17313.
2. Z.-L. Xie, Y. Zhu, J.-Y. Du, D.-Y. Yang, N. Zhang, Q.-Q. Sun, G. Huang and X.-B. Zhang, *Angew. Chem., Int. Ed.*, 2024, **63**, e202400916.
3. K. Lin, Z. He, L. Shen, J. Su, Z. Huang, Y. Xia and Y. Wang, *J. Energy Storage*, 2024, **90**, 111924.
4. P. Luo, Z. Huang, W. Zhang, C. Liu, G. Liu, M. Huang, Y. Xiao, H. Luo, Z. Qu, S. Dong, L. Xia, H. Tang and Q. An, *ChemSusChem*, 2022, **15**, e202200706.
5. Z. Zhao, W. Zhang, M. Liu, D. Wang, X. Wang, L. Zheng, X. Zou, Z. Wang, D. Li, K. Huang and W. Zheng, *Energy Environ. Mater.*, 2023, **6**, e12342.
6. Y. Tan, Z. Chen, Z. Tao, A. Wang, S. Lai, S. Ho and Y. Yang, *Energy Storage Mater.*, 2024, **67**, 103274.
7. T.-U. Wi, C. Park, S. Ko, T. Kim, A. Choi, V. Muralidharan, M. Choi and H.-W. Lee, *Nano Lett.*, 2024, **24**, 7783-7791.
8. C.-Y. Du, Z.-H. Zhang, X.-L. Li, R.-J. Luo, C. Ma, J. Bao, J. Zeng, X. Xu, F. Wang and Y.-N. Zhou, *Chem. Eng. J.*, 2023, **451**, 138650.
9. K. W. Leong, W. Pan, Y. Wang, S. Luo, X. Zhao and D. Y. C. Leung, *ACS Energy Lett.*, 2022, **7**, 2657-2666.
10. C. Li, J. Wu, F. Ma, Y. Chen, L. Fu, Y. Zhu, Y. Zhang, P. Wang, Y. Wu and W. Huang, *ACS Appl. Energy Mater.*, 2019, **2**, 6984-6989.